

# Effect of Anatomical Variability on Neural Stimulation Strength and Focality in Electroconvulsive Therapy (ECT) and Magnetic Seizure Therapy (MST)

Zhi-De Deng, *Student Member, IEEE*, Sarah H. Lisanby, and Angel V. Peterchev, *Member, IEEE*

**Abstract**—We present a quantitative comparison of two metrics—neural stimulation strength and focality—in electroconvulsive therapy (ECT) and magnetic seizure therapy (MST) using finite-element method (FEM) simulation in a spherical head model. Five stimulation modalities were modeled, including bilateral ECT, unilateral ECT, focal electrically administered seizure therapy (FEAST), and MST with circular and double-cone coils, with stimulation parameters identical to those applied in clinical practice. We further examine the effect on the stimulation metrics of individual-, sex- and age-related variability in tissue layer thickness and conductivity. Neural stimulation by MST is shown to be more focal and superficial than ECT. This result suggests that it may be advantageous to reduce the current used in ECT. The stimulation strength in MST is also less sensitive to variations in head geometry and tissue conductivity than in ECT. Individualization of pulse amplitude in both ECT and MST could compensate for anatomical variability, which could lead to more consistent clinical outcomes.

**Index terms**—Magnetic seizure therapy, MST, electroconvulsive therapy, ECT, neural stimulation, electric field, FEM model, variability, depolarization, focality

## I. INTRODUCTION

Electroconvulsive therapy (ECT), in which seizures are electrically induced under anesthesia, is the most effective treatment for severe major depression [1]. However, the use of ECT is limited by cognitive side effects such as amnesia. Magnetic seizure therapy (MST), in which seizures are induced using high dose repetitive transcranial magnetic stimulation (rTMS), offers greater control of the seizure initiation site and a superior side effect profile than ECT [2].

Seizure threshold, defined as the minimum electrical dose necessary to induce an adequate seizure, is used clinically to guide the dosing of ECT [3]. Seizure threshold is determined by administration of electrical pulse trains with increasing duration, frequency, and/or pulse width until a generalized seizure is elicited. Each pulse has fixed current amplitude (typically 800 or 900 mA). Across studies, there is a marked

variability among patients in seizure threshold, with an interindividual range of 40-fold [4]. This large variability is explained only in part by variations in patient characteristics such as age, or treatment factors, such as electrode placement.

It is not known to what extent the age and sex effects on seizure threshold are mediated by interindividual variation in neural excitability and/or anatomy of the head. The induced intracranial electric field, particularly for ECT, is crucially affected by the geometry and electrical conductivities of head tissues. The objective of this study is to quantify the effect of individual-, sex- and age-associated differences in head geometry and conductivity on the induced neural stimulation strength and focality in ECT and MST using finite-element method (FEM) simulation in spherical head models.

Despite the growing interest in FEM simulations with anatomically-accurate, three-dimensional human head models based on structural magnetic resonance imaging (MRI) and diffusion tensor imaging [5],[6], the spherical head model remains widely used in practice. Evidence from physical head model experiments suggest that the spherical model yields good spatial accuracy in electroencephalographic and magnetoencephalographic source localization [7] and has been experimentally validated for transcranial electrical stimulation [8]. Furthermore, in studying the effect of tissue-layer thickness variability, the spherical-shell head model offers an ease of parameterization, which is not straight-forward in a realistic head model. Therefore, in this study we employed a five-layer sphere to represent the human head.

Theoretical and computational comparisons of electric and magnetic stimulation have been presented using spherical [9] and realistic head models [10]. These studies highlighted important differences between electric and magnetic stimulation: the electric field produced by magnetic stimulation is more focal, less penetrating, and insensitive to tissue conductivity compared to electrical stimulation. However, ECT and MST have different pulse shape and width, which result in different levels of neural stimulation for the same electric field magnitude. The above studies did not model this strength-duration effect. In previous work comparing ECT and MST, we accounted for the pulse shape and width, but did not model anatomical variability [11].

The effect of varying cerebrospinal fluid (CSF) thickness and tissue conductivity ratios on the current density distribution in a three-layer spherical model was explored by Stecker [12], who also provided a closed-form, general solution to the Laplace equation in the three-shell sphere. However,

Manuscript received April 7, 2009; revised June 20, 2009. This work was supported in part by grants from NIH NCRR (5TL1RR024158-03), NIMH (R01 MH60884) and NYSTAR.

Z.-D. Deng and A. V. Peterchev are with the Department of Electrical Engineering and with the Division of Brain Stimulation and Therapeutic Modulation, Department of Psychiatry, Columbia University, New York, NY 10032, USA (phone: 212-543-5460; fax: 212-543-4284; email: zd2119@columbia.edu, ap2394@columbia.edu).

S. H. Lisanby is with the Division of Brain Stimulation and Therapeutic Modulation, Department of Psychiatry, Columbia University / New York State Psychiatric Institute, New York, NY 10032, USA (e-mail: slisanby@columbia.edu).

TABLE I PARAMETERS FOR AVERAGE HEAD MODEL

Anatomical parameter	Sex	
	M	F
Head diameter [cm]	17.5	17.3
Scalp thickness [mm]	5.53	5.60
Skull thickness [mm]	6.50	7.08
Cerebrospinal fluid (CSF) thickness [mm]	3.00	3.00
Gray matter (GM) thickness [mm]	3.00	3.00
White matter (WM) thickness [cm]	6.96	6.78
Brain volume [cm <sup>3</sup> ]	1601	1488
Scalp conductivity ( $\sigma_{\text{scalp}}$ ) [S/m]	0.33	
Skull conductivity ( $\sigma_{\text{skull}}$ ) [S/m]	0.0042	
CSF conductivity ( $\sigma_{\text{CSF}}$ ) [S/m]	1.79	
GM conductivity ( $\sigma_{\text{GM}}$ ) [S/m]	0.33	
WM conductivity ( $\sigma_{\text{WM}}$ ) [S/m]	0.14	

Stecker's three-layer spherical model—consisting of skull, CSF, and brain—neglected the presence of the scalp which is critical in determining the amount of current shunting in electrical stimulation. Rath [13] performed parameterizations of tissue layer thicknesses by systematically reducing the thickness of each tissue layer in a four-layer spherical model. This parameterization was only done for the constant-voltage bilateral ECT configuration. No study exists where the effect of anatomical variability of the head is compared between electrical and magnetic stimulation modalities.

In this study, we examine the effect on induced neural stimulation of the variability in head diameter, scalp and skull thicknesses and conductivities, as well as brain volume for five ECT and MST configurations. We provide average, lower, and upper estimates for the induced peak stimulation strength and focality in the adult population.

## II. METHODS

### A. Theory

#### 1) Electrical Stimulation:

Transcranial electrical stimulation produces an electric field that can have both non-zero radial and tangential components. For instance, the electric field has a predominantly radial orientation in the skull due to the significantly lower conductivity of bone relative to the surrounding tissues [14].

#### 2) Magnetic Stimulation:

Unlike electrical stimulation, the electric field induced by magnetic stimulation in a concentric-shell spherical model has no radial component and does not depend on the conductivity of the shells [15],[16]. The tangential component of the electric field is a function of the position within the sphere, as well as the coil geometry, placement and current.

### B. Simulation

Since ECT and MST induce electric fields of relatively low frequencies, the quasistatic approximation can be deployed in electric field models [17]. Under the quasistatic approximation, the electric field solution is separable, that is, it can be expressed as the product of a static electric field amplitude distribution in space,  $E(\mathbf{r})$ , and a time-domain pulse waveform with unit amplitude,  $u(t)$ ,  $E(\mathbf{r}, t) = E(\mathbf{r}) u(t)$ .

#### 1) Electric Field Distribution:

The static electric field distribution,  $E(\mathbf{r})$ , was computed for ECT and MST using the 3D Current Flow and Time

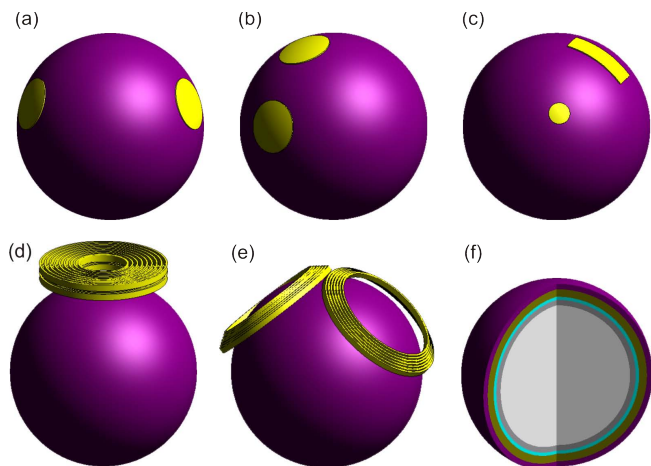


Fig. 1 Simulation models of ECT electrode and MST coil configurations: (a) bilateral ECT (ECT-BL) (b) right unilateral ECT (ECT-RUL), (c) focal electrically administered seizure therapy (ECT-FEAST), (d) MST circular coil (MST-CIRC), (e) MST double-cone coil (MST-DCONE), and (f) interior of the five-layer spherical head model. Tissue layers from outer to inner shell: scalp, skull, CSF, gray matter (GM), and white matter (WM).

Harmonic solvers of the FEM simulation packages ElecNet and MagNet (Infolytica Corp., Montreal, Canada), respectively. The human head was modeled as a five-shell isotropic conducting sphere consisting of the scalp, skull, CSF, gray matter (GM), and white matter (WM), as shown in Fig. 1(f). The nominal values for the tissue layer thicknesses and conductivities were derived from published data (see Sec. II.D) and are given in Table I.

Three ECT electrode configurations [bilateral (BL), right unilateral (RUL), and focal electrically administered seizure therapy (FEAST)] and two MST coil configurations [circular (CIRC) and double-cone (DCONE)] were modeled [illustrated in Fig. 1(a)-(e)]. The electrode and coil geometry, and the stimulation sites and intensities approximated those applied in current clinical practice.

For ECT-BL, two round electrodes with 20-cm<sup>2</sup> area were placed at the frontotemporal position. For ECT-RUL, one electrode was in the right frontotemporal position; the second electrode was placed to the right of vertex [1]. The ECT-FEAST electrode configuration consisted of a large rectangular electrode pad (16 cm<sup>2</sup> area) over the left motor strip and a small circular electrode (3.1 cm<sup>2</sup> area) over the left eyebrow [18]. The ECT electric field was simulated at a current of 800 mA, equal to the output of a MECTA Spectrum 5000Q device (MECTA Corp., Tualatin, OR).

The MST circular coil consisted of two parallel layers of windings, each with an inner diameter of 44 mm, outer diameter of 120 mm, and 9 turns. The double-cone coil consisted of two adjacent windings fixed at a relative angle of 120°, each with an inner diameter of 96 mm, outer diameter of 125 mm, and 7 turns. The circular and double-cone coil inductances,  $L$ , are 22.4  $\mu$ H and 18.41  $\mu$ H, respectively. The coil conductors were placed 7 mm from the surface of the head model to accommodate space for coil casing. The induced electric field magnitude  $E_o(\mathbf{r})$  was solved using an arbitrary coil current  $I_o$  and frequency  $\omega_o$ . The peak electric

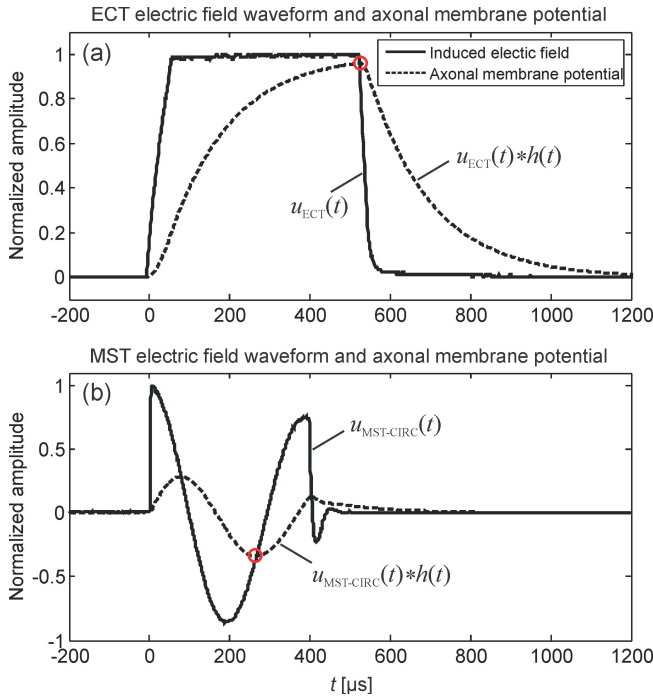


Fig. 2 Recorded electric field waveforms and estimated axonal membrane potentials for (a) ECT and (b) MST with a circular coil. The peaks of the pulse waveforms were normalized to unity. The circles mark the peak change in axonal membrane potential.

field was then scaled to match the output of a Magstim Theta device (Magstim Corp., Whitland, Dyfed, UK):  $E_{MST}(\mathbf{r}) = [E_o(\mathbf{r})/(I_o \omega_o)](V_C/L)$ , where  $V_C = 1.65$  kV is the peak capacitor voltage.

## 2) Pulse Waveform:

The ECT electric field waveform,  $u_{ECT}(t)$ , is proportional to the electrode current waveform. The ECT waveform was recorded from a MECTA Spectrum 5000Q set to pulse width of 0.5 ms [see Fig. 2(a)]. The MST electric field waveforms,  $u_{MST-CIRC}(t)$  [see Fig. 2(b)] and  $u_{MST-DCONE}(t)$  (not shown), were recorded with a search coil from a Magstim Theta with circular and double-cone coils, respectively.

## C. Neural Stimulation Metrics

### 1) Peak Stimulation Strength

Electric and magnetic stimulation modeling studies often report peak electric field (or current density) to quantify the strength of neural stimulation. However, it is well known that the neural response depends also on the pulse shape and width, due to the neuronal membrane capacitance. Thus, the threshold electric field amplitude to induce neural response depends on the pulse shape and width; this dependence is often expressed as a strength-duration relation [19]. Therefore, we propose that the more appropriate metric to quantify the strength of stimulation is the electric field amplitude,  $E(\mathbf{r})$ , relative to the neural response threshold,  $E_{th}$ , for the given pulse shape and width, i.e.,  $E(\mathbf{r})/E_{th}$ .

The threshold electric field,  $E_{th}$ , is typically derived empirically. For example, the threshold electric field to induce motor response (the motor threshold, MT) is approximately 0.85 V/cm for the Magstim 200 TMS stimulator with a fig-

ure-8 coil (Magstim Corp.) [20]-[22]. Stimulation at 40% above MT (1.2 V/cm) produces robust neural activation with motor evoked potential amplitude of approximately 90% of maximum [23]. These thresholds are specific to the Magstim 200 electric field waveform which has a damped cosine shape. To estimate the corresponding electric field thresholds for other pulse shapes and widths, we have to consider a model of the neuronal membrane response to stimulation.

To first order, the neuronal membrane can be modeled as a low-pass filter with time constant  $\tau_m$  [24]. Therefore, the change in membrane potential resulting from an electric field pulse,  $E(\mathbf{r}, t)$ , is

$$\begin{aligned} \Delta V_m(\mathbf{r}, t) &= \gamma E(\mathbf{r}, t) * h(t) \\ &= \gamma E(\mathbf{r}) u(t) * h(t) \end{aligned} \quad (1)$$

where ‘\*’ is the convolution operator;  $h(t)$  is the impulse response of a low-pass filter with time constant  $\tau_m$ . It is thought that the axon is the neural element preferentially depolarized by extracellular electric field stimulation, therefore it can be assumed that  $\tau_m = 150$   $\mu$ s [24],[25]. The constant  $\gamma$  characterizes the membrane depolarization sensitivity to electric field and is approximately 66 mV per V/cm [26]. Thus,  $u(t) * h(t)$  is proportional to the axonal membrane depolarization; it is plotted with dashed line in Fig. 2 together with the corresponding  $u(t)$  for an ECT and an MST pulse.

Regardless of the pulse shape, the neuron will fire when  $\Delta V_m$  reaches an approximately constant threshold level. Therefore, by equating  $\Delta V_m$  at threshold for two pulse shapes,  $u_1(t)$  and  $u_2(t)$ , we obtain the following relationship between the corresponding threshold electric field amplitudes

$$\frac{E_{th1}}{E_{th2}} = \frac{\max(|u_2(t) * h(t)|)}{\max(|u_1(t) * h(t)|)}. \quad (2)$$

The quantity  $\max(|u(t) * h(t)|)$  is 0.96, 0.34, and 0.30 for ECT, MST-CIRC, and MST-DCONE, respectively. For a Magstim 200 with figure-8 coil,  $\max(|u(t) * h(t)|) = 0.25$  and  $E_{th} = 1.2$  V/cm for robust neural response, as noted above. Using these values together with Eq. (2), we can estimate the thresholds to be  $E_{th,ECT} = 0.31$  V/cm,  $E_{th,MST-CIRC} = 0.89$  V/cm, and  $E_{th,MST-DCONE} = 1.0$  V/cm. These values are based on the neural response threshold for motor cortex, since there are scarce data for other brain areas. If the threshold and membrane time constant for other brain areas are known, they can be used in the analysis above. Using these estimated thresholds, we can compute the relative stimulation strength metric  $E(\mathbf{r})/E_{th}$ .

### 2) Focality:

We quantified the stimulation focality by the percentage of gray and white matter volume that is exposed to an electric field strong enough to produce suprathreshold depolarization in the majority of neurons, i.e. the volume where  $E(\mathbf{r})/E_{th} \geq 100\%$ .

## D. Head Anatomical Parameters

### 1) Head Diameter:

The diameters of the head models were based on the weighted average of adult male and female measurements for head circumference reported in [27],[28]. The upper and

TABLE II PEAK STIMULATION STRENGTH AND STIMULATED VOLUME FOR AVERAGE HEAD MODELS

Sex	Peak stimulat. strength relative to neural response threshold [%]										Volume stimulated above neural response threshold [%]									
	ECT					MST					ECT					MST				
	BL		RUL		FEAST		CIRC		DCONE		BL		RUL		FEAST		CIRC		DCONE	
	GM	WM	GM	WM	GM	WM	GM	WM	GM	WM	GM	WM	GM	WM	GM	WM	GM	WM	GM	WM
M	429	521	474	471	488	541	124	110	230	207	100	100	72	90	73	90	9.4	0.5	18	5.5
F	413	493	441	439	466	505	120	106	222	199	100	100	69	88	70	89	10	0.7	21	5.9

TABLE III VARIABILITY OF PEAK STIMULATION STRENGTH AND STIMULATED VOLUME

Anatomical parameter	Sex	Parameter variation [%]	Peak stimulation strength change [%]										Stimulated volume change [%]									
			ECT					MST					ECT					MST				
			BL		RUL		FEAST		CIRC		DCONE		BL		RUL		FEAST		CIRC		DCONE	
			GM	WM	GM	WM	GM	WM	GM	WM	GM	WM	GM	WM	GM	WM	GM	WM	GM	WM	GM	WM
Head diameter	M	+8.3	-2.7	2.7	4.4	4.6	3.4	5.6	2.6	2.4	5.9	5.3	0	0	-5.5	-5.1	-7.2	-6.3	-7.0	6.9	12	7.6
	F	-13	6.3	-0.9	-6.3	-6.7	-2.7	-4.4	-4.0	-5.4	-10	-11	0	0	10	6.8	18	8.8	8.5	-32	-21	-3.7
Scalp thickness	M	+6.4	-3.1	0.6	2.0	1.9	0.6	1.2	1.6	2.1	4.9	3.9	0	0	-5.1	-4.6	-6.7	-5.5	-4.3	4.7	21	1.4
	F	-13	5.4	-1.3	-6.3	-6.8	-3.5	-5.1	-4.4	-4.7	-9.6	-10.4	0	0	8.8	7.1	16	9.1	5.2	-63	-13	-4.8
Skull thickness	M	+32	-15	-16	-18	-18	-19	-20	-6.8	-7.0	-4.5	-4.5	0	0	-23	-13	-23	-13	-22	-73	-16	-13
	F	-58	51	59	74	73	76	82	13	12	8.5	8.3	0	0	36	11	33	11	30	166	25	28
Brain volume	M	+21	-11	-12	-13	-13	-14	-15	-3.2	-3.2	-2.5	-3.3	0	0	-19	-10	-19	-9.7	-11	-55	-10	-8.9
	F	-38	29	32	39	38	39	42	8.4	7.9	6.0	5.1	0	0	31	12	30	11	25	144	22	18
σ <sub>skull</sub>	M	+34	-13	-15	-17	-17	-18	-17	-8.3	-8.5	-5.5	-5.6	0	0	-20	-11	-19	-9.8	-13	-60	-10	-11
	F	-26	14	16	20	20	20	23	17	17	4.4	4.2	0	0	14	6.1	13	5.5	68	1033	28	22
σ <sub>scalp</sub>	M	+34	-14	-15	-17	-17	-17	-19	-8.9	-8.5	-5.4	-6.2	0	0	-24	-13	-23	-12	-31	-100	-9.0	-9.6
	F	-26	15	17	21	21	21	23	19	18	5.4	4.4	0	0	18	7.7	17	6.9	67	885	34	27
σ <sub>skull</sub>	M	-5	-14	-16	-17	-17	-17	-17	-4.8	-5.3	-4.5	-4.3	0	0	-21	-13	-21	-13	-14	-53	-16	-9.1
	F	-15	-33	-36	-38	-38	-38	-38	-15	-14	-12	-12	0	0	-54	-41	-52	-39	-59	-100	-34	-26
σ <sub>scalp</sub>	M	-5	-14	-15	-16	-16	-16	-18	-4.6	-3.9	-3.4	-2.9	0	0	-24	-15	-24	-14	-15	-74	-12	-8.6
	F	-15	-33	-35	-37	-37	-37	-39	-14	-13	-11	-11	0	0	-55	-43	-54	-41	-80	-100	-27	-26
σ <sub>skull</sub>	M	+319	74	96	120	119	122	139	0	0	0	0	0	0	31	11	27	9.7	0	0	0	0
	F	-74	-58	-61	-65	-65	-65	-65	0	0	0	0	-32	-1.3	-85	-86	-83	-83	0	0	0	0
σ <sub>scalp</sub>	M	-25	18	20	23	23	23	24	0	0	0	0	0	0	23	9.7	21	8.6	0	0	0	0
	F	-50	43	52	61	61	61	65	0	0	0	0	0	0	42	13	38	12	0	0	0	0

lower limits corresponded to two standard deviations above and below the means in [27] and [28], respectively.

2) Scalp Thickness:

The scalp thicknesses of the head models were a weighted average of the measurements reported in [29],[30]. The upper and lower limits were taken from [30] and [29], respectively.

3) Skull Thickness:

While some morphometric studies suggest no significant sex difference in cranium thickness [31]-[33], a recent study by Li et al. based on computed tomography (CT) head scans of a large population of living subjects showed women having significantly thicker skulls than men [34]. The skull thicknesses of our head models were based on averaging the frontal, parietal and occipital bone measurements reported in [34]. The upper and lower limits of the models corresponded to the 10<sup>th</sup> and 90<sup>th</sup> percentile measurements. It should be noted that Li et al. collected the CT scans from only one city in China, the data may not be representative of skull geometric variation for other populations.

4) Brain Volume:

Structural MRI estimates of peripheral CSF and brain volume show significantly greater cortical atrophy in elderly men compared to women [35]-[37]. The decrease in volume at the frontal, temporal and parieto-occipital lobes can be as large as 15% in elderly men compared to 4% in women [35]-[37]. In this study, we examined the effect of shrinking the total brain volume (gray and white matter) by 5% and by 15% in both the male and female head models. The skull shell

diameter was kept constant and the CSF volume was increased to fill the vacated space within the cranium.

5) Skull Conductivity:

A gray-matter-to-skull conductivity ratio of 80 is the most commonly used in the neural source localization literature [38],[39]. Recently, a series of *in vivo* measurements showed that this conductivity ratio should be lower [40]-[42]. There is no evidence of sex difference in skull conductivity, although the data are too sparse to draw any firm conclusions [40]-[43]. Therefore, we varied the skull conductivity only in the male model. The upper limit of the GM-to-skull conductivity ratio is taken to be 290 [44], and the lower limit is taken to be 18.7 [41]. More sophisticated skull models have multi-layer structure and/or anisotropy [45]. However, boundaries between the spongiosa and the compacta layers of the skull are often difficult to determine on MRI scans [6],[45], therefore, in this study we modeled the skull as a single layer.

6) Scalp Conductivity:

The available literature on sex difference in scalp conductivity is even more limited than that for the cranium. Baysal and Hauelsen estimated the scalp resistivity in four adult male and five adult female subjects [43]; the small sample showed no systematic difference between men and women.

Scalp conductivity would be expected to depend on the composition of its constituent layers. It has been observed that the hypodermis, which makes up about 50% of the scalp cross section, is thicker in women than in men [29]. Since this fat-storing layer has higher impedance than skin and muscle [46], it is conceivable that women would have lower overall

scalp conductivity compared to men. To examine the effect of reduced scalp conductivity on the induced stimulation strength, we simulated a 25% and 50% decrease in scalp conductivity in the female head model.

### III. RESULTS

The simulation results for peak stimulation strength relative to threshold and focality corresponding to the five stimulation modalities are summarized in Tables II and III.

#### A. Average Head Model

The results for the average head models are given in Table II. All forms of ECT induced similar stimulation strength in the gray matter (superficial brain) and white matter (deeper brain) ranging from 413% to 541% of threshold, whereas values for MST-CIRC and MST-DCONE were much lower, ranging from 106% to 207% of threshold. With ECT-BL and ECT-FEAST, stimulation strength was higher in white matter than gray matter, while the reverse pattern was seen in MST.

Stimulated volume was much higher with ECT than MST (up to 100% for ECT, and up to 21% for MST). Of note, ECT-BL stimulated 100% of gray and white matter. ECT-RUL and ECT-FEAST stimulated a higher volume of white than gray matter, while with MST the reverse pattern was seen. The stimulated volume for ECT-RUL and ECT-FEAST were similar.

Men and women showed a similar pattern of effects in both stimulation strength and stimulated volume.

#### B. Effect of Anatomical Variation

The effect of tissue layer thickness and conductivity variation is summarized in Table III. Head diameter variability has the least effect compared to variability in other parameters. Variations in scalp and skull thickness, as well as in brain volume have larger effects on stimulation strength in ECT (up to 82% increase in WM stimulation strength for ECT-FEAST) compared to MST (up to 19% increase in GM stimulation strength for MST-CIRC).

Stimulation strength was slightly less affected by tissue dimension and conductivity variations in ECT-BL compared to ECT-RUL and ECT-FEAST, which were similar. MST-DCONE tended to be less sensitive to anatomical variations than MST-CIRC. The volume stimulated by MST-CIRC was highly sensitive to the changes in tissue dimensions.

Finally, variation in skull and scalp conductivity has no effect on the stimulation strength or focality for MST.

### IV. DISCUSSION AND CONCLUSIONS

#### A. Electrical vs. Magnetic Stimulation

Our simulation results indicate that MST provides more focal stimulation than ECT, i.e., the stimulated gray matter and white matter volumes for MST-CIRC and MST-DCONE are less than those in ECT (Table II). This observation is consistent with previous findings [9],[11], and was part of the original motivation for the development of MST [47]. For ECT, large portions of the brain (up to 100% with ECT-BL) are being stimulated at high intensities relative to neuronal threshold (up to 541% with ECT-FEAST). A more focal and

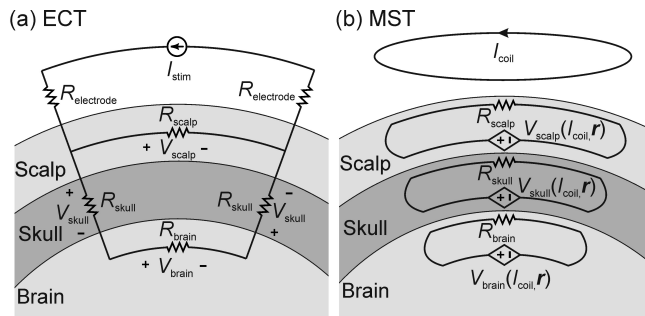


Fig. 3 Simplified, lumped-circuit models of the electric field induced by (a) ECT, (b) MST. These models provide insight into the relative insensitivity to anatomical variations of MST compared to ECT.

less intense form of seizure induction may reduce the side effects of ECT, as seen with MST [2]. These observations suggest that using lower current amplitudes and/or briefer pulses could improve the focality of ECT and provide stimulation closer to the physiological thresholds, which may improve safety.

MST is more confined to the superficial cortex than ECT, consistent with previous simulation studies [11],[12] and with *in vivo* data [48], which may be important for limiting side effects. The relative stimulation strength and the stimulated volume of gray matter are higher than those in the white matter for MST. The opposite pattern was observed for ECT due to the relatively lower conductivity of white matter compared to gray matter.

The ECT-FEAST paradigm was proposed to achieve more focal seizure induction [49]. We found no substantial difference between ECT-FEAST and ECT-RUL in stimulation strength or stimulated brain volume. However, ECT-FEAST and ECT-RUL also differ in electric field localization and orientation, which were not evaluated in this study.

#### B. Differential Impact of Anatomical Variation

Peak stimulation strength is less sensitive to variability of scalp, skull, and brain properties in MST compared to ECT. This effect was hypothesized in the original motivation for MST development [47]. Here we present the first quantitative verification of this hypothesis.

To understand the insensitivity of MST to anatomical variation, we can consider the simplified, lumped-circuit models of ECT and MST given in Fig. 3. As discussed in Sec. II.A, magnetic stimulation induces a purely tangential electric field that is independent of conductivity. As shown in Fig. 3 (b), the induced electric field is represented by voltage sources that depend on the coil current  $I_{coil}$  and position  $r$ . The effective resistances connected to the voltage sources represent the tissue impedance that is inversely proportional to the conductivity. The impedances of CSF, GM and WM are lumped into a single parameter  $R_{brain}$  for simplicity. Clearly, in each tissue layer, for a given  $I_{coil}$  and position  $r$ , the induced voltage (and hence the electric field and stimulation strength) does not depend on the local conductivity or the properties of the other layers. Varying the thickness of the tissue layers in MST amounts to changing the coil-to-cortex distance, which, in turn, leads to variation in the induced



electric field magnitude. On the other hand, an analogous lumped-circuit model for ECT [Fig. 3(a)] reveals that the induced voltages depend on the local conductivity and on the overall current distribution in the head which is a function of the properties of all the layers [4].

On the other hand, Table III suggests that the brain volume stimulated by MST-CIRC is highly sensitive to the changes in tissue dimensions. This is due to the high focality (small nominal stimulated volume) of MST-CIRC which leads to small absolute changes in stimulated volume resulting in large percentage changes.

The sensitivity of stimulation strength and focality to anatomical differences could result in undesirable interindividual variability in clinical outcomes. The commonly used seizure-threshold titration procedure adjusts the duration and/or frequency of the stimulus pulse train, but not pulse amplitude [3],[4]. While titration in the frequency and duration domains addresses the time-dependent behavior of the brain, it fails to account for the anatomy-dependent variability in the strength and spatial extent of direct neural stimulation which is driven by pulse amplitude. To control for this variability, pulse amplitude could be individualized, e.g. based on a patient-specific electric field simulation, or by setting the amplitude relative to the patient's motor threshold, as is conventionally done in clinical rTMS [50].

### C. Sex-Related Effects

While sex is a predictor of seizure threshold in ECT [3], sex was not a major determinant of stimulation strength or focality in this study. Sackeim et al. attributed the lower seizure threshold in women to their thinner skull thickness resulting in less current shunting [4]. This argument was based on skull thickness measurements in children (age 6 to 16) [51]. One study in adults has found the skull to be thicker in women than in men [34], resulting in lower electric field strength in the female brain. When varying the skull thickness in our models, we have kept the GM-to-skull conductivity ratio constant at 80, an assumption that may not be accurate. Tang et al. found a negative correlation between skull resistivity and thickness [52]. This correlation should be included in future simulation studies.

It has been asserted that the sex difference in scalp composition would also contribute to the seizure threshold variation, though no supporting evidence was cited [4]. It has been shown that women have thicker hypodermis than men [29]. This could effect lower scalp conductivity in women, resulting in less current shunting during ECT, stronger stimulation strength and larger stimulated brain volume (see Table III), and, consequently, lower seizure threshold.

### D. Age-Related Effects

After the age of 18, the cranium does not show significant increase in thickness with age [34],[53]. Therefore, we do not expect a large age-dependent effect on the induced electric field variation from the growth in skull thickness in adults.

The hypodermis thickness does not undergo significant change with aging in men, whereas changes in hypodermis thickness in women covaried with estrogen level during the

lifetime [54]. In addition to structural changes that accompany hormonal fluctuations, estrogen is also known to increase the number of hippocampal excitatory neuron synapses and increase seizure susceptibility in female epileptic patients [55].

Brain atrophy is a large source of variability in stimulation focality for ECT. A 15% decrease in brain volume led to a 55% decrease in stimulated gray matter volume in ECT-RUL. This effect is consistent with the repeated observation that seizure threshold increases with age [56],[57].

### E. Limitations

The spherical model has obvious shortcomings: the head is not perfectly spherical; tissue layers have non-uniform thickness, and heterogeneous and anisotropic conductivities; and the skull has orifices such as the auditory and optic canals, representing low-impedance paths for electrical current. A refinement of this study could use more anatomically accurate head models. However, any single realistic head model cannot be used to reliably capture the anatomical variability of the population. Furthermore, varying the thicknesses of individual tissue layers is not straightforward with a realistic head model. The spherical model is valuable in quantifying anatomical variability effects in ECT and MST that could be subsequently explored in more realistic models.

## V. REFERENCES

- [1] S. H. Lisanby, "Electroconvulsive therapy for depression," *N Engl J Med*, vol. 357, pp. 1939-1945, 2007.
- [2] S. H. Lisanby, B. Luber, T. E. Schlaepfer, and H. A. Sackeim, "Safety and feasibility of magnetic seizure therapy (MST) in major depression: Randomized within-subject comparison with electroconvulsive therapy," *Neuropsychopharm* vol. 28, pp. 1852-1865, 2003.
- [3] H. A. Sackeim, P. Decina, I. Prohvnik, and S. Malitz, "Seizure threshold in electroconvulsive therapy: effects of sex, age, electrode placement, and number of treatments," *Arch Gen Psychiat*, vol. 44, pp. 355-360, 1987.
- [4] H. A. Sackeim, J. Long, B. Luber, J. R. Moeller, I. Prohvnik, D. P. Devanand, and M. S. Nobler, "Physical properties and quantification of ECT stimulus: I. Basic principles," *Convuls Ther*, vol. 10, pp. 93-123, 1994.
- [5] M. Chen and D. J. Mogul, "A structurally detailed finite element human head model for simulation of transcranial magnetic stimulation," *J Neurosci Meth*, vol. 179, pp. 111-120, 2009.
- [6] C. H. Wolters, A. Anwander, X. Tricoche, D. Weinstein, M. A. Koch, and R. S. MacLeod, "Influence of tissue conductivity anisotropy on EEG/MEG field and return current computation in a realistic head model: A simulation and visualization study using high-resolution finite element modeling," *NeuroImage*, vol. 30, pp. 813-826, 2006.
- [7] B. N. Cuffin, "Eccentric spheres models of the head," *IEEE Trans Biomed Eng*, vol. 38, pp. 871-878, 1991.
- [8] S. Rush and D. A. Driscoll, "Current distribution in the brain from surface electrodes," *Anesth Anal*, vol. 47, pp. 717-723, 1968.
- [9] J. M. Saypol, B. J. Roth, L. G. Cohen, and M. Hallett, "A theoretical comparison of electric and magnetic stimulation of the brain," *Ann Biomed Eng*, vol. 19, pp. 317-328, 1991.
- [10] M. Nadeem, T. Thorlin, O. P. Gandhi, and M. A. Persson, "Computation of electric and magnetic stimulation in human head using the 3-D impedance method," *IEEE Trans Biomed Eng*, vol. 50, pp. 900-907, 2003.
- [11] Z.-D. Deng, A. V. Peterchev, and S. H. Lisanby, "Focality of neural stimulation with magnetic seizure therapy (MST) and electroconvulsive therapy (ECT) in humans and non-human primates," in *64th Ann Conv Soc Biol Psychiatry*, Vancouver, Canada, 2009.
- [12] M. M. Stecker, "Transcranial electric stimulation of motor pathways: a theoretical analysis," *Comput Biol Med*, vol. 35, pp. 133-155, 2005.

- [13] W. T. Rath, "Modeling of transcranial electrical stimulation by finite element analysis," in *Department of Bioengineering*. vol. Master of Science: University of Pittsburgh, 2006.
- [14] P. C. Miranda, M. Lomarev, and M. Hallett, "Modeling the current distribution during transcranial direct current stimulation," *Clin Neurophysiol*, vol. 117, pp. 1623-1629, 2006.
- [15] D. Cohen and B. N. Cuffin, "Developing a more focal magnetic stimulator. Part I: Some basic principles," *J Clin Neurophysiol*, vol. 8, pp. 102-111, 1991.
- [16] H. Eaton, "Electric field induced in a spherical volume conductor from arbitrary coils: application to magnetic stimulation and MEG," *Med Biol Eng Comp*, vol. 30, pp. 433-440, 1992.
- [17] B. J. Roth, L. G. Cohen, M. Hallett, W. Friauf, and P. J. Basser, "A theoretical calculation of the electric field induced by magnetic stimulation of a peripheral nerve," *Muscle Nerve*, vol. 13, pp. 734-741, 1990.
- [18] T. Spellman, A. V. Peterchev, and S. H. Lisanby, "Focal electrically administered seizure therapy: A novel form of ECT illustrates the roles of current directionality, polarity, and electrode configuration in seizure induction," *Neuropsychopharm*, vol. 34, pp. 2002-2010, 2009.
- [19] L. A. Geddes, "Optimal stimulus duration for extracranial cortical stimulation," *Neurosurgery*, vol. 20, pp. 94-99, 1987.
- [20] D. Rudiak and E. Marg, "Finding the depth of magnetic brain stimulation: a re-evaluation," *Electroenceph Clin Neurophysiol*, vol. 93, pp. 358-371, 1994.
- [21] C. M. Epstein, D. G. Schwartzberg, K. R. Davey, and D. B. Sudderth, "Localizing the site of magnetic brain stimulation in humans," *Neurology*, vol. 40, pp. 666-670, 1990.
- [22] A. Thielscher and T. Kammer, "Linking physics and physiology in TMS: A sphere field model to determine the cortical stimulation site in TMS," *NeuroImage*, vol. 17, pp. 1117-1130, 2002.
- [23] J. B. Pitcher, K. M. Ogston, and T. S. Miles, "Age and sex differences in human motor cortex input-output characteristics," *J Physiol*, vol. 546, pp. 605-613, 2003.
- [24] A. T. Barker, C. W. Garnham, and I. L. Freeston, "Magnetic nerve stimulation: the effect of waveform on efficiency, determination of neural membrane time constants and the measurement of stimulator output," *Electroenceph Clin Neurophysiol Suppl*, vol. 43, pp. 227-237, 1991.
- [25] L. G. Nowak and J. Bullier, "Axons, but not cell bodies, are activated by electrical stimulation in cortical gray matter I. Evidence from chronaxie measurements," *Exp Brain Res*, vol. 118, pp. 477-488, 1998.
- [26] T. Radman, R. L. Ramos, J. C. Brumberg, and M. Bikson, "Targets of cortical electrical stimulation: Layer 5 pyramidal neurons," in *Conf Proc Neural Interfaces*, 2008.
- [27] A. R. Örmeci, H. Gürbüz, A. Ayata, and H. Çetin, "Adult head circumferences and centiles," *J Turgut Özal Med Cent*, vol. 4, pp. 261-264, 1997.
- [28] K. Y. Manjunath, "Estimation of cranial volume in dissecting room cadavers," *J Anat Soc India*, vol. 51, pp. 168-172, 2002.
- [29] H. Hori, G. Moretti, A. Rebora, and F. Crovato, "The thickness of human scalp: normal and bald," *J Invest Derm*, vol. 58, pp. 396-399, 1972.
- [30] A. J. Lupin and R. J. Gardiner, "Scalp thickness in the temporal region: its relevance to the development of cochlear implants," *Coch Imp Int*, vol. 2, pp. 30-38, 2001.
- [31] A. H. Ross, R. L. Jantz, and W. F. McCormick, "Cranial thickness in American females and males," *J Forensic Sci*, vol. 43, pp. 267-272, 1998.
- [32] P. Smith, Y. Wax, A. Becker, and S. Einy, "Diachronic variation in cranial thickness of Near Eastern populations," *Am J Phys Anthropol*, vol. 67, pp. 127-133, 1985.
- [33] M. S. Buchsbaum, R. I. Henkin, and R. L. Christiansen, "Age and sex differences in averaged evoked responses in a normal population, with observations on patients with gonadal dysgenesis," *Electroenceph Clin Neurophysiol*, vol. 37, pp. 137-144, 1974.
- [34] H. Li, J. Ruan, Z. Xie, H. Wang, and W. Liu, "Investigation of the critical geometric characteristics of living human skulls utilising medical image analysis techniques," *Int J Vehicle Safety*, vol. 2, pp. 345-367, 2007.
- [35] C. E. Coffey, J. F. Lucke, J. A. Saxton, G. Ratcliff, L. J. Unitas, B. Billig, and R. N. Bryan, "Sex differences in brain aging: A quantitative magnetic resonance imaging study," *Arch Neurol*, vol. 55, pp. 169-179, 1998.
- [36] P. E. Cowell, B. I. Turetsky, R. C. Gur, R. I. Grossman, D. L. Shtasel, and R. E. Gur, "Sex differences in aging of the human frontal and temporal lobes," *J Neurosci*, vol. 14, pp. 4748-4755, 1994.
- [37] D. G. Murphy, C. DeCarli, A. R. McIntosh, E. Daly, M. J. Mentis, P. Pietrini, K. Szczepanik, M. B. Schapiro, C. L. Grady, B. Horwitz, and S. I. Rapoport, "Sex differences in human brain morphometry and metabolism: an in vivo quantitative magnetic resonance imaging and positron emission tomography study on the effect of aging," *Arch Gen Psychiat*, vol. 53, pp. 585-594, 1996.
- [38] S. Rush and D. A. Driscoll, "EEG electrode sensitivity--an application of reciprocity," *IEEE Trans Biomed Eng*, vol. 16, pp. 15-22, 1969.
- [39] S. Homma, T. Musha, Y. Nakajima, Y. Okamoto, S. Blom, R. Flink, and K.-E. Hagbarth, "Conductivity ratios of the scalp-skull-brain head model in estimating equivalent dipole sources in human brain," *Neurosci Res*, vol. 22, pp. 51-55, 1995.
- [40] T. F. Oostendorp, J. Delbeke, and D. F. Stegeman, "The conductivity of the human skull: results of in vivo and in vitro measurements," *IEEE Trans Biomed Eng*, vol. 47, pp. 1487-1491, 2000.
- [41] Y. Zhang, W. van Drongelen, and B. He, "Estimation of in vivo brain-to-skull conductivity ratio in human," *Appl Phys Lett*, vol. 89, pp. 223903-223903, 2006.
- [42] Y. Lai, W. van Drongelen, L. Ding, H. E. Hecox, V. L. Towle, D. M. Frim, and B. He, "Estimation of in vivo human brain-to-skull conductivity ratio by means of cortical potential imaging," *IJBEM*, vol. 7, pp. 311-312, 2005.
- [43] U. Baysal and J. Hauseisen, "Use of a priori information in estimating tissue resistivities--application to human data in vivo," *Physiol Meas*, vol. 25, pp. 737-748, 2004.
- [44] K. J. Eriksen, "In vivo human head regional conductivity estimation using a three-sphere model," in *Conf Proc IEEE Eng Med Biol Soc*, 1990, pp. 1494-1495.
- [45] R. J. Sadleir and A. Argibay, "Modeling skull electrical properties," *Ann Biomed Eng*, vol. 35, pp. 1699-1712, 2007.
- [46] X. Zhao, Y. Kinouchi, E. Yasuno, D. Gao, T. Iritani, T. Morimoto, and M. Takeuchi, "A new method for noninvasive measurement of multilayer tissue conductivity and structure using divided electrodes," *IEEE Trans Biomed Eng*, vol. 51, pp. 362-370, 2004.
- [47] H. A. Sackeim, "Magnetic stimulation therapy and ECT," *Convuls Ther*, vol. 10, pp. 255-258, 1994.
- [48] S. H. Lisanby, T. D. Moscrip, O. Morales, B. Luber, C. Schroeder, and H. A. Sackeim, "Neurophysiological characterization of magnetic seizure therapy (MST) in non-human primates," in *Transcranial Magnetic Stimulation and Transcranial Direct Current Stimulation (Supplements to Clinical Neurophysiology)*. vol. 56, W. Paulus, F. Tergau, M. A. Nitsche, J. C. Rothwell, U. Ziemann, and M. Hallett, Eds.: Elsevier Science, 2003.
- [49] H. A. Sackeim, "Convulsant and anticonvulsant properties of electroconvulsive therapy: towards a focal form of brain stimulation," *Clin Neurosci Res*, vol. 4, pp. 39-57, 2004.
- [50] E. M. Wassermann, "Risk and safety of repetitive transcranial magnetic stimulation: report and suggested guidelines from the International Workshop on the Safety of Repetitive Transcranial Magnetic Stimulation, June 5-7, 1996," *Electroenceph Clin Neurophysiol*, vol. 108, pp. 1-16, 1998.
- [51] M. L. Riolo, R. E. Moyers, J. A. J. McNamara, and W. S. Hunter, *An Atlas of Craniofacial Growth*. Ann Arbor: University of Michigan, 1974.
- [52] C. Tang, F. You, G. Cheng, D. Gao, F. Fu, G. Yang, and X. Dong, "Correlation between structure and resistivity variation of the live human skull," *IEEE Trans Biomed Eng*, vol. 55, pp. 2286-2292, 2008.
- [53] T. W. Todd, "Thickness of the male white cranium," *Anat Rec*, vol. 27, pp. 245-256, 1927.
- [54] K. Pedersen-Bjergaard and M. Tønnesen, "Oestrogenic, androgenic and gonadotrophic substances in the urine of normal women; sex hormone analyses," *Acta Endocrinol*, vol. 1, pp. 38-60, 1948.
- [55] C. S. Woolley, "Acute effects of estrogen on neuronal physiology," *Annu Rev Pharmacol Toxicol*, vol. 47, pp. 657-680, 2007.
- [56] C. E. Coffey, J. Lucke, R. D. Weiner, A. D. Krystal, and M. Aque, "Seizure threshold in electroconvulsive therapy: I. Initial seizure threshold," *Biol Psychiat*, vol. 37, pp. 713-720, 1995.
- [57] J. D. Tew, B. H. Mulsant, R. F. Haskett, J. Prudic, M. E. Thase, R. R. Crowe, D. Dolata, A. E. Begley, C. F. Reynolds, and H. A. Sackeim, "Acute efficacy of ECT in the treatment of major depression in the old-old," *Am J Psychiatry*, vol. 156, pp. 1865-1870, 1999.